PHYSICAL REVIEW D **89,** 093017 (2014)

Electron events from the scattering with solar neutrinos in the search of keV scale sterile neutrino dark matter

Wei Liao, Xiao-Hong Wu, and Hang Zhou

Institute of Modern Physics, School of Sciences, East China University of Science and Technology, 130 Meilong Road, Shanghai 200237, People's Republic of China

(Received 29 November 2013; published 21 May 2014)

In a previous work, we showed that it is possible to detect keV scale sterile neutrino dark matter ν_s in a β decay experiment using radioactive sources such as ^{3}T or ^{106}Ru. The signals of this dark matter candidate are monoenergetic electrons produced in the neutrino capture process $\nu_s + N' \to N + e^-$. These electrons have energy greater than the maximum energy of the electrons produced in the associated decay process $N' \to N + e^- + \bar{\nu}_e$. Hence, signal electron events are well beyond the end point of the β decay spectrum and are not polluted by the β decay process. Another possible background, which is a potential threat to the detection of ν_s dark matter, is the electron event produced by the scattering of solar neutrinos with electrons in target matter. In this article, we study in detail this possible background and discuss its implications for the detection of keV scale sterile neutrino dark matter. In particular, bound state features of electrons in Ru atoms are considered with care in the scattering process when the kinetic energy of the final electron is the same order of magnitude of the binding energy.

DOI: 10.1103/PhysRevD.89.093017 PACS numbers: 14.60.Pq, 13.15.+g

I. INTRODUCTION

Among many dark matter (DM) candidates, keV scale sterile neutrino warm DM is a very interesting possibility. It has several virtues. Included among them are (1) it is capable of smoothing the structure of the Universe at a small scale and reducing the overabundance of small scale structures observed in the simulation of cold DM scenarios [1]; (2) it provides a fermionic dark matter candidate with an appropriate mass scale which naturally avoids the cusp core in the halo density profile [2]; (3) it naturally gives a lifetime longer than the age of the Universe and does not need to include by hand a discrete or global symmetry to guarantee the stability or long lifetime of the DM [3,4]; and (4) it is easy to get such a DM candidate in well-motivated models such as the seesaw models [5,6] which are the most popular models for explaining the tiny masses of active neutrinos.

Many aspects of this warm DM candidate, e.g., the production mechanism in the early Universe [5,7–11], the astrophysical and cosmological constraints, possible models and symmetries, etc., have been analyzed and considered [12–24] model independently or in special models. Among them, attention has been paid to the detection of this keV scale DM. It was realized that indirect detection of this DM background in the Universe to a good sensitivity can be achieved in principle using satellite observation of monoenergetic x rays produced in two-body decay of the DM: $\nu_s \to \nu + \gamma$. However, this observation scheme requires large statistics which is not available in the present scale satellite observation program [25]. Direct detection of this DM candidate in the laboratory has also been investigated [3,4,26–30]. Because of its small mass and weak interaction, some authors found it impossible to detect this DM candidate in the laboratory [27–30].

In a previous work, we proposed that keV scale ν_s DM can be detected using β decay nuclei such as ^{3}T and ^{106}Ru [3]. It was found that with a small mixing with the electron neutrino ν_e, ν_s can be captured by ^{3}T and ^{106}Ru in the process $\nu_s + N' \to N + e^-$. The signals of ν_s DM are monoenergetic electrons with energy well beyond the end point of the β decay spectrum. It was shown in [3] that the signal electrons produced in the ν_s capture process have kinetic energy $Q_\beta + m_{\nu_s}$, where m_{ν_s} is the mass of ν_s. Q_β is the decay energy of the decay process $N' \to N + e^- + \bar{\nu}_e$. Q_β is equal to the maximal kinetic energy of electrons produced in the decay process, i.e., the kinetic energy at the end point of the decay spectrum. For ^{106}Ru, $Q_\beta = 39.4$ keV. For ^{3}T, $Q_\beta = 18.59$ keV. So for $m_{\nu_s} \approx 1$–2 keV, the signal electrons have kinetic energy around 20 keV for ^{3}T and around 40 keV for ^{106}Ru, respectively. We found that with a reasonable amount of ^{3}T and ^{106}Ru as a target, we can get a few to tens of signal electrons per year for the mixing angle squared θ^2 around 10^{-6}. This estimate of the event rate is only constrained by the constraint on the mixing angle from x-ray observation of the sterile neutrino decay [3,12,13,31]: $\theta^2 < 1.8 \times 10^{-5}(\mathrm{keV}/m_{\nu_s})^5$. This constraint only assumes that the sterile neutrino DM accounts for all of the DM in the Universe and is independent of models of sterile neutrino DM. For models in which sterile neutrino DM is a part of all DM in the Universe, this constraint is weaker. Hence, we concluded that detection of keV scale sterile neutrino DM is possible using this detection scheme. More details and general features of this detection scheme have been further analyzed in [26].

Two kinds of background electron events have also been discussed in [3]. One type of background event is generated when radioactive nuclei ^{3}T or ^{106}Ru capture solar electron neutrinos of energy around keV and produce final electrons in an energy range close to that of the ν_s capture process. These electrons can mimic the signal electron of ν_s DM. Fortunately, this type of background is sufficiently small because solar neutrino flux at the keV energy range is pretty small. Another possible background event occurs when electrons are kicked out by neutrinos in the scattering of solar neutrinos with electrons in target matter. This type of background should be discussed in detail, which was not done in detail in [3], however, for the following reasons: (1) solar neutrinos with higher energy can also participate in the scattering process and the total solar neutrino flux contributing to the background events is significantly higher than that for the first type of background; and (2) since signal electrons have an energy of tens keV, which is the same order of magnitude of the binding energy of the electrons in the inner shell of ^{106}Ru atoms, the bound state feature of initial electrons in the scattering process should be taken into account at least for the scattering with electrons in the inner shell of ^{106}Ru atoms.

In this article, we will discuss in detail the scattering of neutrinos with bound state electrons. Attention will be paid to the scattering of neutrinos with electrons in the inner shell of Ru atoms and the events of final electrons with energy of tens keV. We will analyze the detailed energy distribution of the scattering of neutrinos with bound state electrons. We will discuss the dependence of the scattering process on the neutrino energy. We will analyze electron events caused by the scattering with solar neutrinos and the limitations for the detection of keV scale sterile neutrino DM. In the following, we will first review the bound state feature of electrons in ^{106}Ru and discuss some general features of the scattering of neutrinos with bound electrons. Then we will come to detailed discussions of the scattering of neutrinos with electrons in ^{106}Ru. Finally, we will discuss the events of the scattering of solar neutrinos with bound state electrons and discuss the implications for DM detection.

II. ELECTRONS IN ^{106}Ru ATOMS AND THEIR INTERACTION WITH NEUTRINOS

In this section we briefly review features of bound electrons in ^{106}Ru atoms and discuss some general features of the scattering of neutrinos with bound electrons. For reasons to be explained below, we will not discuss in detail the scattering with bound electrons in ^{3}T atoms.

As noted above, the signal electrons produced in the ν_s DM capture process, $\nu_s + N' \to N + e^-$, have kinetic energy $Q_\beta + m_{\nu_s}$. For a keV scale ν_s DM with a mass of 1–2 keV, the signal electrons have kinetic energy around 20 keV for ^{3}T and 40 keV for ^{106}Ru, respectively.

The atomic number of the ruthenium element is 44. In Table I, we list the electronic levels of the ground state configuration of neutral ruthenium atoms [32] and the corresponding binding energies obtained from x-ray data [32,33]. One can see that electrons in the K and L shells have binding energies greater than keV. When considering final electrons with energy around 40 keV, one would expect that bound state features may have some effects on the scattering of neutrinos with electrons at these energy levels. We would also expect that the effect of the bound state features in the scattering with electrons in the L shell should be weaker than that in the scattering with electrons in the K shell.

For the scattering with electrons in the M, N, and O shells in Ru atoms, we expect that bound state features of these electrons should not give a large correction to the neutrino-electron scattering of interest to us. As noted above, we would be interested in the events of electrons with energy around 40 keV. As can be seen in Table I, this energy is at least about 2 orders of magnitude larger than the binding energy of electrons in the M, N, and O shells. Detailed studies, to be given in the following, show that even effects of the bound state feature of the electrons in the L shell are not large in the energy range $\gtrsim$40 keV. These studies support what we expect for the scattering with electrons in the M, N, and O shells.

For ^{3}T, the binding energy is the famous 13.6 eV. It is 3 orders of magnitude smaller than the kinetic energy of interest to us, say $\sim$20 keV. Similar to the discussion above for the electrons in the M, N, and O shells of Ru atoms, it is natural to expect that bound state features of the initial electrons in ^{3}T should not have a significant effect on the neutrino-electron scattering process when discussing events with final electrons of an energy around 20 keV.

To understand in detail the scattering of neutrinos with bound electrons in Ru atoms, we need the wave function of the bound electron. Neglecting relativistic corrections, interactions of nonrelativistic electrons in an atom include interaction with the nucleus through a central force and the interaction with other electrons. The Hamiltonian for such a system can be written as

TABLE I. Ground state configuration of neutral Ru atoms and the binding energy from x-ray experiments [32,33].

Electronic level	K	L_I	L_{II}	L_{III}	M_I	M_{II}	M_{III}	M_{IV}	M_V	N_I	N_{II}	N_{III}	N_{IV}	N_V	O_I
State	$1s$	$2s$	$2p_{\frac{1}{2}}$	$2p_{\frac{3}{2}}$	$3s$	$3p_{\frac{1}{2}}$	$3p_{\frac{3}{2}}$	$3d_{\frac{3}{2}}$	$3d_{\frac{5}{2}}$	$4s$	$4p_{\frac{1}{2}}$	$4p_{\frac{3}{2}}$	$4d_{\frac{3}{2}}$	$4d_{\frac{5}{2}}$	$5s$
No. of electrons	2	2	2	4	2	2	4	4	6	2	2	4	4	3	1
Binding E (keV)	22.1	3.22	2.97	2.84	0.59	0.48	0.46	0.28	0.28	0.075	0.043	0.043	0.002	0.002	⋯

$$\mathcal{H} = \sum_i \frac{\hat{p}_i^{\,2}}{2m_e} - \sum_i \frac{Ze^2}{r_i} + \sum_{i<j} \frac{e^2}{r_{ij}}, \tag{1}$$

where $\hat{p}_i$ is the momentum operator of the ith electron, r_i the radius of the ith electron, r_{ij} the distance between the ith electron and jth electrons, e the charge of electron, and Z the atomic number. It is very difficult to solve states of electrons including all details of these interactions. Fortunately, one can take the approximation that the forces of all other electrons acting on a single electron can be approximated as a mean central force, and the state of a single electron can be solved using an effective Hamiltonian

$$\mathcal{H}_i = \frac{\hat{p}_i^{\,2}}{2m_e} - \frac{Ze^2}{r_i} + V_i(r_i), \tag{2}$$

where V_i arises from the interaction of the ith electron with all other electrons. A further approximation one can use is that the effect of an electron in an outer shell on an electron in an inner shell can be taken as small, since the distance between these electrons can be considered large compared to distances between electrons in the inner shell.

For an electron in the K shell of a Ru atom, the above approximation works well. According to the approximation described above, an electron in the K shell is similar to an electron in the ground state of the hydrogen atom except that the atomic number is replaced by $Z = 44$. Using this approximation, the binding energy of an electron in the K shell is estimated to be $\varepsilon = m_e Z^2\alpha^2/2$, where α is the fine structure constant. Using this approximation for an electron in the K shell of a Ru atom, we find that $\varepsilon \approx 26.3$ keV, which is consistent with the binding energy from x-ray data shown in Table I. This convinces us that the wave function of an electron in the K shell of a Ru atom can be approximated as the one similar to the wave function of the $1s$ state in a hydrogen atom. In momentum space, this wave function can be written as

$$\varphi_{1s}(p) = \frac{2\sqrt{2}}{\pi} \frac{a_K^{3/2}}{(p^2 a_K^2 + 1)^2}. \tag{3}$$

It satisfies

$$\int d^3p |\varphi_{1s}(p)|^2 = 1. \tag{4}$$

Equation (3) is normalized to give a kinetic energy $1/(2m_e a_K^2)$, where a_K is the effective radius of the electron in the state of the K shell. The binding energy equals the kinetic energy $\varepsilon_K = 1/(2m_e a_K^2)$, as a consequence of the Virial theorem. So a_K can be determined using the binding energy shown in Table I. When using only the central force from the interaction with the nucleus, one has $a_K = 1/(m_e Z\alpha)$ and one can recover the previous estimate: $\varepsilon_K = m_e Z^2\alpha^2/2$.

For electrons in the L shell of a Ru atom, the above approximation also seems to work well. The evidence is the quasidegeneracy of binding energies of L_I, L_{II}, and L_{III} states, as shown in Table I. One can see that the binding energies of these energy levels are almost the same. This suggests that the dynamical $SO(4)$ symmetry works well for electrons in these states and the mean potentials acted on these electrons should be close to a $1/r$ law. So the wave functions of electrons in the L level can be approximated as those similar to the $2s$ and $2p$ wave functions in the hydrogen atom. In momentum space, we write these wave functions as

$$\varphi_{2s}(p) = \frac{a_L^{3/2}}{\pi} \frac{p^2 a_L^2 - 1/4}{(p^2 a_L^2 + 1/4)^3}, \tag{5}$$

$$\varphi_{2p0}(p) = -\frac{i a_L^{3/2}}{\pi} \frac{p_z a_L}{(p^2 a_L^2 + 1/4)^3}, \tag{6}$$

$$\varphi_{2p\pm1}(p) = \frac{a_L^{3/2}}{\sqrt{2}\pi} \frac{(p_x \pm i p_y) a_L}{(p^2 a_L^2 + 1/4)^3}, \tag{7}$$

where $2pi (i = 0, \pm 1)$ refers to states with different projections of angular momentum onto the z direction. These wave functions satisfy

$$\int d^3p |\varphi_l(p)|^2 = 1, \qquad l = 2s, 2p0, 2p+1, 2p-1. \tag{8}$$

They are normalized to give a kinetic energy $1/(2^3 m_e a_L^2)$. The binding energy is equal to the kinetic energy $\varepsilon_L = 1/(2^3 m_e a_L^2)$, as a consequence of the Virial theorem. So a_L can be determined using the binding energy shown in Table I. For simplicity, we use a universal ε_L for all $2s$ and $2p$ states in definitions given in Eqs. (5), (6), and (7).

For electrons in the M, N, and O shells, the situation is a bit complicated. As can be seen in Table I, there are no quasidegeneracies of states in the M, N, and O shells. Fortunately, these states have much smaller binding energies than the states in the K and L shells. In particular, their binding energies are about 2 orders of magnitude smaller than the energy range of the kinetic energy of scattered electrons, i.e., $\gtrsim$40 keV, which is of interest to us. We would expect that the bound state features of electrons in these states should not alter the scattering process significantly, and we should be able to approximate these electrons as at rest with the energy equal to the rest mass.

III. SCATTERING OF NEUTRINOS WITH BOUND ELECTRON IN RU ATOM

For the scattering of a neutrino with a free electron at rest, the cross section is well known [34]:

$$\frac{d\sigma_0}{dE_k} = \frac{G_F^2 m_e}{2\pi}\left[(g_V+g_A)^2 + (g_V-g_A)^2\left(1-\frac{E_k}{E_\nu}\right)^2 - (g_V^2-g_A^2)\frac{E_k m_e}{E_\nu^2}\right], \tag{9}$$

where E_ν is the energy of the initial neutrino, E_k the kinetic energy of the scattered electron, and $g_{V,A}$ are the vector and axial-vector coupling constants [34]. $g_V = -\frac{1}{2} + 2\sin^2\theta_W$ and $g_A = -\frac{1}{2}$ for the muon and tau neutrino. For the electron neutrino, $g_V = \frac{1}{2} + 2\sin^2\theta_W$, $g_A = \frac{1}{2}$. θ_W is the weak mixing angle with $\sin^2\theta_W = 0.231$. The kinetic energy of the scattered electron lies in the range

$$E_k \subset [0, E_\nu/(1+m_e/(2E_\nu))]. \tag{10}$$

One can see in Eq. (9) that the differential cross section varies slowly with respect to E_k.

For the scattering of a neutrino with a bound electron in a Ru atom, the neutrino directly transfers energy and momentum to the electron. The neutrino neither affects the other parts of the atom nor is it affected by the other parts of the atom. This is exactly the case in which the impulse approximation works [35]. Furthermore, we can approximate the wave function of the scattered electron as the plane wave. This is because we would concentrate on the energy range, $\gtrsim$40 keV, for the scattered electron. For kinetic energy larger than the binding energy, one can take the plane wave approximation for the wave function of the scattered electrons [35].

The scattering of a neutrino with bound electrons should in principle be treated in a relativistic framework. This requirement would give rise to complication when taking into account the relativistic wave function of an electron in a bound state. Fortunately, we can simplify the discussion by noticing that the electrons in Ru atoms can be considered nonrelativistic, as can be seen in Table I. Furthermore, the spin-orbit coupling is zero for electrons in the K shell which have zero angular momentum, and the energy shift due to the spin-orbit coupling to electrons in the L shell should have a negligible effect on our result for the events with scattered electrons of $E_k \gtrsim 40$ keV. So we can approximately take spin and angular momentum as independent variables, as in the case of nonrelativistic quantum mechanics. In this approximation, the total wave function of the bound electron can be approximated as a product of a spinor and a wave function in x or p coordinates:

$$\Psi(\vec{x}) = \psi\phi(\vec{x}), \qquad \Phi(\vec{p}) = \psi\varphi(\vec{p}), \tag{11}$$

where ψ is a spinor and it is equal to $(1,0,0,0)^T$ or $(0,1,0,0)^T$ in the standard Dirac representation of spinors.

In this approximation, one can find that the cross section of the scattering of a neutrino with an electron in a particular state l can be written as

$$\frac{d\sigma_l}{dE_k} = \int d^3p_B |\varphi_l(\vec{p}_B)|^2 \frac{d\sigma_{\vec{p}_B}}{dE_k}, \tag{12}$$

where E_k is the kinetic energy of the final electron, and $\sigma_{\vec{p}_B}$ the cross section of the scattering of a neutrino with an electron of energy $E_B = m_e - \varepsilon$ and momentum $\vec{p}_B$. Equation (12) says that the neutrino has a probability, $|\varphi_l(\vec{p}_B)|^2 d^3p_B$, to scatter with an electron carrying momentum $\vec{p}_B$, and the cross section is a sum of contributions of the scattering with electrons carrying all possible $\vec{p}_B$'s.

The energy and momentum conservation conditions for $\sigma_{\vec{p}_B}$ are

$$E_\nu + E_B = E'_\nu + E_e, \qquad \vec{p}_\nu + \vec{p}_B = \vec{p}'_\nu + \vec{p}_E, \tag{13}$$

where E_B is the energy of a bound electron as given above, E_e the energy of the final electron, E_ν the energy of the initial neutrino, E'_ν the energy of the final neutrino, $\vec{p}_\nu$ the momentum of the initial neutrino, $\vec{p}'_\nu$ the momentum of the final neutrino, and $\vec{p}_E$ the momentum of the final electron. Using Eq. (11), one can find that

$$\frac{d\sigma_{\vec{p}_B}}{dE_k} = \frac{G_F^2}{4\pi^2|\vec{p}_{\nu B}|}\int_0^{2\pi} d\phi \frac{1}{2}\sum_{\text{spin}}|\mathcal{M}|^2, \tag{14}$$

where $\vec{p}_{\nu B} = \vec{p}_\nu + \vec{p}_B$, ϕ is the azimuthal angle of $\vec{p}_E$ with respect to the axis of $\vec{p}_{\nu B}$, and

$$\frac{1}{2}\sum_{\text{spin}}|\mathcal{M}|^2 = (g_V+g_A)^2 p'_\nu\cdot p_E + (g_V-g_A)^2 p_\nu\cdot p_E\frac{E'_\nu}{E_\nu} - (g_V^2-g_A^2)\frac{m_e}{E_\nu}p_\nu\cdot p'_\nu. \tag{15}$$

p_ν, p'_ν, p_E are the four-momenta of the initial neutrino, final neutrino, and final electron, respectively. In Eq. (15), an average over the spin of the initial electron has been performed.

Using Eq. (13), one can find that

$$p'_\nu\cdot p_E = \frac{1}{2}(E_T^2 - |\vec{p}_{\nu B}|^2 - m_e^2), \tag{16}$$

$$2\vec{p}_{\nu B}\cdot\vec{p}_E = |\vec{p}_{\nu B}|^2 + |\vec{p}_E|^2 - (E_T - E_e)^2, \tag{17}$$

where $E_T = E_\nu + E_B$ is the total energy of the scattering process. One can see that the projection of $\vec{p}_E$ onto the axis of $\vec{p}_{\nu B}$ is fixed by the energy-momentum conservation condition, but the azimuthal angle ϕ is not fixed. Using Eq. (17), one can easily find that

$$\frac{1}{2\pi}\int_0^{2\pi} d\phi\,\vec{p}_E = \vec{p}_{\nu B}S, \tag{18}$$

where

$$S = \frac{|\vec{p}_{\nu B}|^2 + |\vec{p}_E|^2 - (E_T - E_e)^2}{2|\vec{p}_{\nu B}|^2}. \quad (19)$$

Using Eq. (18), one can find that

$$\frac{d\sigma_{\vec{p}_B}}{dE_k} = \frac{G_F^2}{2\pi|\vec{p}_{\nu B}|}\frac{1}{2}\sum_{\text{spin}}|\tilde{M}|^2, \quad (20)$$

where

$$\begin{aligned}\frac{1}{2}\sum_{\text{spin}}|\tilde{M}|^2 = {} & \frac{1}{2}(g_V + g_A)^2(E_T^2 - |\vec{p}_{\nu B}|^2 - m_e^2) \\ & + (g_V - g_A)^2(E_\nu E_e - \vec{p}_\nu \cdot \vec{p}_{\nu B} S)\frac{E'_\nu}{E_\nu} \\ & - (g_V^2 - g_A^2)\frac{m_e}{E_\nu}[E_\nu(E_T - E_e) \\ & - \vec{p}_\nu \cdot \vec{p}_{\nu B}(1 - S)]. \end{aligned} \quad (21)$$

For $\vec{p}_B = 0$ and $E_B = m_e$, one can easily show that Eq. (20) recovers Eq. (9).

Using Eq. (13), one can find that the energies of the final electron and final neutrino lie in the following range:

$$E_e \subset \left[\frac{(E_T - |\vec{p}_{\nu B}|)^2 + m_e^2}{2(E_T - |\vec{p}_{\nu B}|)}, \frac{(E_T + |\vec{p}_{\nu B}|)^2 + m_e^2}{2(E_T + |\vec{p}_{\nu B}|)}\right] \quad (22)$$

$$E'_\nu \subset \left[\frac{E_T^2 - |\vec{p}_{\nu B}|^2 - m_e^2}{2(E_T + |\vec{p}_{\nu B}|)}, \frac{E_T^2 - |\vec{p}_{\nu B}|^2 - m_e^2}{2(E_T - |\vec{p}_{\nu B}|)}\right]. \quad (23)$$

A number of comments follow:

(A) From Eqs. (17), (22), and (23), one can read out that not all electrons with all possible $\vec{p}_B$'s can contribute to the cross section. Some $\vec{p}_B$ range is forbidden due to kinematical constraint. $\vec{p}_B$'s that are allowed to contribute to the scattering process should satisfy

$$E_T^2 - |\vec{p}_{\nu B}|^2 - m_e^2 \geq 0. \quad (24)$$

If $E_T^2 - m_e^2 \leq 0$, no $\vec{p}_B$ range can contribute to the kinematically allowed range and the process is forbidden. This is just the threshold condition for the process to happen, i.e., $E_\nu > \varepsilon$.

(B) From Eqs. (22) and (23) one can read out that the energy ranges of the final particles depend on $|\vec{p}_{\nu B}|$. The total width of the range of electron energy is

$$\Delta E_e = E_e|_{\max} - E_e|_{\min} = \frac{E_T^2 - |\vec{p}_{\nu B}|^2 - m_e^2}{E_T^2 - |\vec{p}_{\nu B}|^2}|\vec{p}_{\nu B}|. \quad (25)$$

(C) One can check in Eq. (22) that the minimum of the energy of the final electron is larger than or equal to m_e. To allow the energy range to reach m_e requires

$$E_T - |\vec{p}_{\nu B}| = m_e. \quad (26)$$

This requires that $\vec{p}_B$ lie in a very narrow range. Hence, the differential cross section for the $E_k \approx 0$ range is suppressed by a factor arising from the momentum distribution of $\vec{p}_B$: $|\varphi(\vec{p}_B)|^2\delta^3 p_B$.

(D) From Eq. (22), one can show that $E_e|_{\max}$ increases with $|\vec{p}_{\nu B}|$. Using Eq. (24), one can find out the maximum energy of the final electron in the scattering process:

$$E_e \leq \frac{1}{2}\left(E_T + \sqrt{E_T^2 - m_e^2} + \frac{m_e^2}{E_T + \sqrt{E_T^2 - m_e^2}}\right) = E_T. \quad (27)$$

As a comparison, we can find in Eq. (10) that for the scattering with the free electron at rest, the maximum energy of the final electron is $\frac{1}{2}[m_e + 2E_\nu + m_e^2/(m_e + 2E_\nu)]$. For $E_\nu \gg \varepsilon$, we can easily figure out that the energy of the final electron extends beyond the range allowed by the scattering with the free electron at rest.

(E) Equations (12) and (20) appear to be singular for $|\vec{p}_{\nu B}| \to 0$. This is an artificial singularity. As can be seen in Eq. (25), the energy range of the final electron shrinks also as $|\vec{p}_{\nu B}| \to 0$. This cancels the singular term in Eqs. (12) and (20) in the integrated cross section. Furthermore, one can see that $|\vec{p}_{\nu B}| \approx 0$ corresponds to a very narrow range of $\vec{p}_B$. In numerical calculation, the contribution to the differential cross section of electrons in this narrow range can be easily controlled by taking it as $|\varphi(\vec{p}_B)|^2\delta^3 p_B \Delta E_e/|\vec{p}_{\nu B}|\frac{1}{2}G_F^2|\tilde{M}|^2/(2\pi)$. Using Eq. (25), one can see that it is suppressed by the factor $|\varphi(\vec{p}_B)|^2\delta^3 p_B$, and in practice one can neglect it by taking a small enough range of $\delta^3 p_B$.

IV. NUMERICAL RESULTS AND DISCUSSION

In Fig. 1, we show the differential cross section for the scattering of an electron neutrino with an electron in the K shell of a Ru atom. One can see that at the $E_k \approx 0$ tail, the differential cross section drops down sharply. As a comparison, one can see that the cross section of the scattering with a free electron at rest remains constant for $E_k = 0$. As noted in comment (C) above, this is because the initial electron has a distribution of momentum and the probability of finding the electron in the required momentum range, i.e., the range for reaching $E_k \approx 0$, is small.

In Fig. 1, we can see that the scattering of a neutrino with a bound electron has an E_k spectrum wider than that of the scattering with a free electron at rest. As shown in Eq. (10), the kinetic energy of the final electron in the scattering with a free electron at rest lies in a limited range with a maximum value which can be much smaller than E_ν when $E_\nu < m_e$. In contrast, the final electron is allowed to get a kinetic energy as large as $E_\nu - \varepsilon$ for the scattering with a bound electron, as noted in comment (D) above. One can

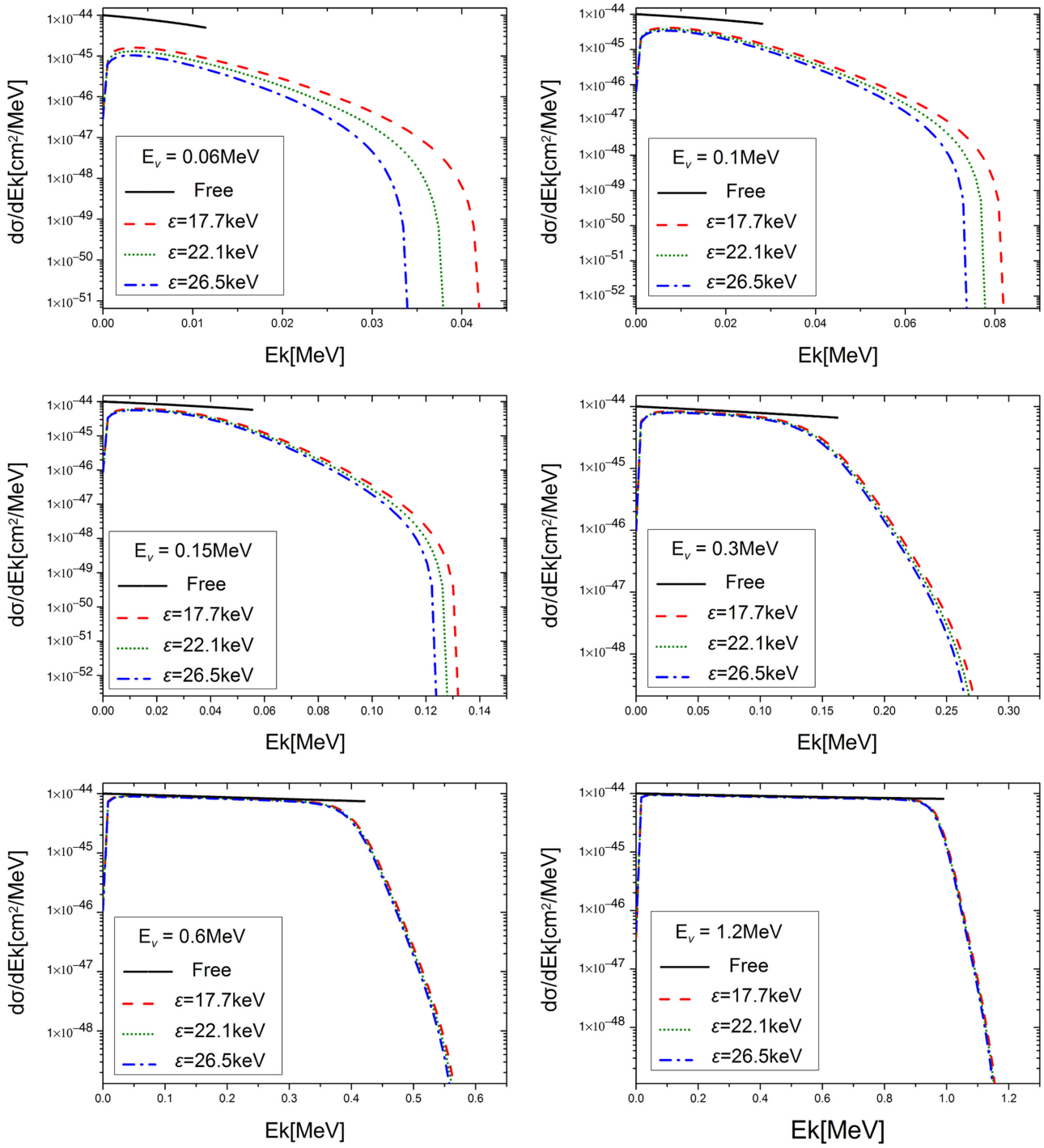

FIG. 1 (color online). Differential cross section of the scattering of an electron neutrino with a bound electron in the K shell of a Ru atom. The black solid line is for the scattering with an electron at rest with E_k in the kinematically allowed range $[0, E_\nu/(1 + m_e/(2E_\nu))]$. The three colored lines are for $\varepsilon = 17.7$, 22.1, 26.5 keV, respectively.

find that for $E_\nu \lesssim 0.15$ MeV, the difference between the allowed energy ranges of the scattering with a free electron and the scattering with a bound electron is very large. For $E_\nu > m_e$, the difference becomes negligible.

One can see in Fig. 1 that for large E_ν, the cross section of the scattering with a bound electron becomes close to that of the scattering with a free electron at rest. In particular, for $E_\nu \gtrsim 0.3$ MeV, the cross section of the scattering with a bound electron agrees well with that of the free electron case in the kinematically allowed region of E_k in the free electron case. Although there is still a tail beyond the range allowed by the scattering with a free

electron at rest, the differential cross section in the tail region is suppressed by several orders of magnitude.

As a comparison, we plot three lines in Fig. 1 for $\varepsilon = 22.1$ keV and $\pm 20\%$ variation of this value of binding energy. One can see that 20% variation does not lead to a large difference for the scattering with $E_\nu > 0.1$ MeV. It has an impact on the scattering with $E_\nu = 0.06$ MeV. In particular, there are visible differences close to the end of the tails in the plot for $E_\nu = 0.06$ MeV. This corresponds to the change of the threshold for the production of a final electron with a particular energy. It is not a surprise that this threshold would depend on the value of ε.

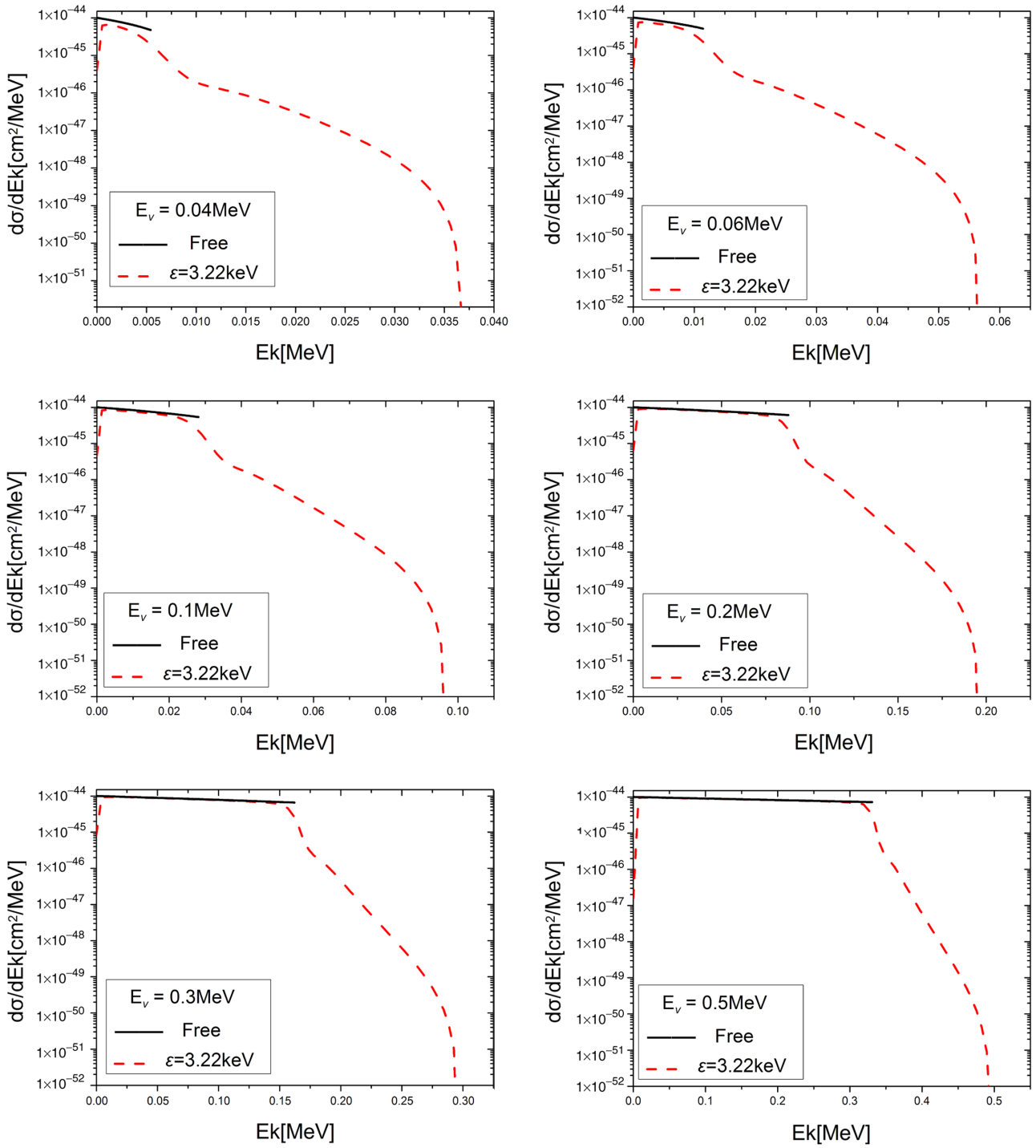

FIG. 2 (color online). Differential cross section of the scattering of an electron neutrino with a bound electron in the $2s$ state of a Ru atom. The black solid line is for the scattering with an electron at rest with E_k in the kinematically allowed range $[0, E_\nu/(1 + m_e/(2E_\nu))]$. The binding energy is chosen as $\varepsilon = 3.22$ keV.

In Fig. 2, we plot the differential cross section of the scattering of an electron neutrino with an electron in the $2s$ state. We can find phenomena similar to that discussed above for the scattering with an electron in the $1s$ state. A major difference is that the lines for the scattering with an electron in the $2s$ state get close to that of the free electron case at smaller E_ν compared to the lines of the scattering with an electron in the $1s$ state. One can see in Fig. 2 that for $E_\nu \gtrsim 0.06$ MeV, the differential cross section of the scattering with a bound electron is already quite close to

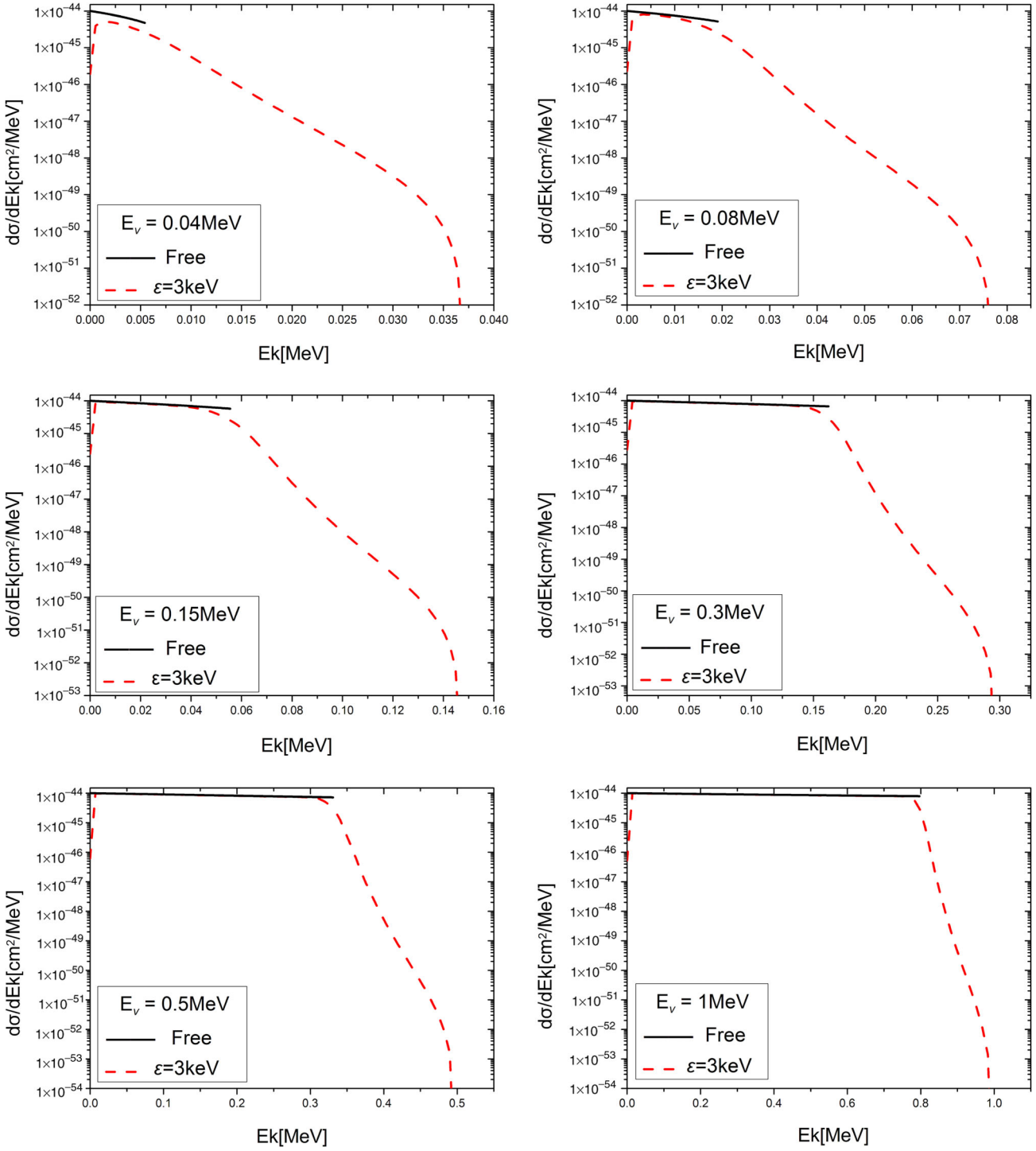

FIG. 3 (color online). Differential cross section of the scattering of an electron neutrino with a bound electron in the $2p$ state of a Ru atom. The black solid line is for the scattering with an electron at rest with E_k in the kinematically allowed range $[0, E_\nu/(1 + m_e/(2E_\nu))]$. The binding energy is chosen as $\varepsilon = 3$ keV.

that of the scattering with a free electron in the energy range, $[0, E_\nu/(1+m_e/(2E_\nu))]$, allowed by the scattering with a free electron.

In Fig. 3, we plot the differential cross section of the scattering of an electron neutrino with an electron in the $2p$ state of a Ru atom. The plot is given for the cross section evaluated for the average momentum distribution $|\varphi_{2p}|^2$ of electrons in the $2p$ state:

$$\frac{d\sigma_{2p}}{dE_k} = \int d^3p_B |\varphi_{2p}(\vec{p}_B)|^2 \frac{d\sigma_{\vec{p}_B}}{dE_k}, \tag{28}$$

where

$$|\varphi_{2p}(\vec{p}_B)|^2 = \frac{1}{3}(|\varphi_{2p0}(\vec{p}_B)|^2 + |\varphi_{2p+1}(\vec{p}_B)|^2 + |\varphi_{2p-1}(\vec{p}_B)|^2). \tag{29}$$

For convenience, we choose a universal binding energy $\varepsilon_L = 3$ keV for φ_{2p0} and $\varphi_{2p\pm1}$. We note that $2p_{\frac{1}{2}}$ and $2p_{\frac{3}{2}}$ states correspond to linear combinations of φ_{2p0} and $\varphi_{2p\pm1}$ together with spinors. An advantage of computing Eq. (28) is that it is invariant after the recombination of wave functions φ_{2p0} and $\varphi_{2p\pm1}$. In particular, computation using $2p_{\frac{1}{2}}$ and $2p_{\frac{3}{2}}$ wave functions leads to the same result as in Eq. (29) after averaging the contributions of all the electrons in the $2p_{\frac{1}{2}}$ and $2p_{\frac{3}{2}}$ states.

In Fig. 3, we can find phenomena similar to that discussed for the scattering with an electron in the $2s$ state. Similarly, we can find in Fig. 3 that for $E_\nu \gtrsim 0.06$ MeV, the differential cross section of the scattering with a bound electron is already quite close to that of the scattering with a free electron in the energy range, $[0, E_\nu/(1+m_e/(2E_\nu))]$, allowed by the scattering with a free electron at rest.

We have seen in Figs. 1–3 that the final electron has an energy range wider than that for the scattering with a free electron at rest. In particular, one can show that neutrinos with energy $E_\nu < \frac{1}{2}(E_k + \sqrt{E_k^2 + 2E_k m_e})$ do not contribute to the differential cross section, Eq. (9), for a fixed $E_k > 0$. While considering electron events of a particular kinetic energy E_k, one finds that some low energy neutrinos in the initial spectrum do not contribute to these types of events when using the cross section of the scattering with a free electron at rest. According to the above discussion, these low energy neutrinos can indeed contribute to these types of events when using the cross section of the scattering with a bound electron.

In Fig. 4, we plot the differential cross section for $E_k = 42$ keV versus the initial E_ν. One can see in Fig. 4 that for the scattering of an electron neutrino with a free electron, the cross section starts to be nonzero from a nonzero value of E_ν, which is $(E_k + \sqrt{E_k^2 + 2m_e E_k})/2$ as discussed above. For the scattering with a bound electron, the cross section starts to be nonzero from a much smaller value of E_ν than that of the scattering with a free electron at rest.

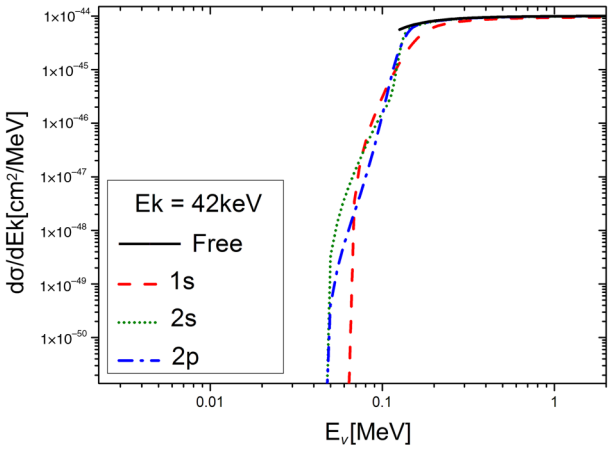

FIG. 4 (color online). Differential cross section versus E_ν, the energy of the initial neutrino, for the scattering of an electron neutrino with a bound electron in a Ru atom. The binding energies for $1s$, $2s$, and $2p$ states are chosen the same as in Figs. 1, 2, and 3, respectively. The energy of the final electron is fixed as $E_k = 42$ keV.

For E_ν close to the threshold value, the differential cross section of the scattering with bound electrons can start from a value infinitely close to zero. One can see that the lines for the scattering with electrons in the $2s$ or $2p$ states are very close to the line for the scattering with a free electron at rest in the kinematically allowed energy range of the scattering with a free electron. Outside of this allowed energy range, the cross sections of the scattering with electrons in the $2s$ or $2p$ states decrease sharply for orders of magnitude. This means that the bound state features of $2s$ and $2p$ states just give small corrections to the scattering process. For comparison, one can see that the line for the scattering with an electron in the $1s$ state is not very close to the line for the free electron case. There are visible differences between the line for the free electron case and the line for the electron in the $1s$ state up to $E_\nu \sim 0.2$–0.3 MeV. In Fig. 5, we give a plot similar to Fig. 4 except for the scattering of muon neutrinos with bound electrons. One can see phenomena similar to that in Fig. 4.

In Figs. 4 and 5, we have seen that the cross section of the scattering with bound electrons in the L shell ($2s$ or $2p$ states) agrees well with the cross section of the scattering with a free electron at rest, and the bound state features give small corrections to the scattering process. It is natural to expect that the bound state features of electrons in the M, N, and O shells should give even smaller corrections compared to those of the electrons in the L shell. This is easy to understand because the binding energies of states in these shells are much smaller than those of the states in the L shell, as can be seen in Table I. According to this discussion, we can approximate the cross section of the scattering with electrons in the M, N, and O shells as that of the scattering with a free electron at rest.

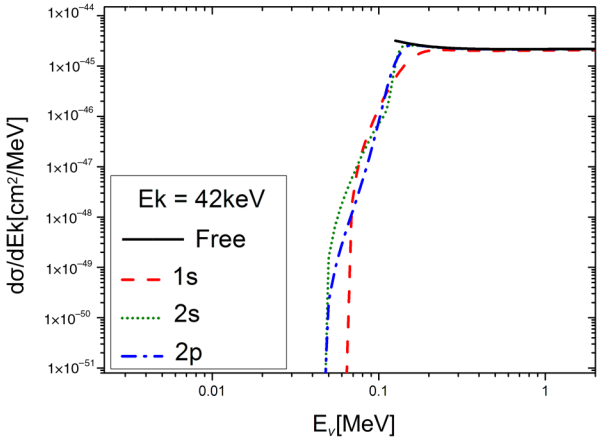

FIG. 5 (color online). Differential cross section versus E_ν, the energy of the initial neutrino, for the scattering of a muon neutrino with a bound electron in a Ru atom. The binding energies for $1s$, $2s$, and $2p$ states are chosen the same as in Figs. 1, 2, and 3, respectively. The energy of the final electron is fixed as $E_k = 42$ keV.

V. SCATTERING OF SOLAR NEUTRINO WITH BOUND ELECTRON IN RU ATOM

Solar neutrinos are electron neutrinos produced in fusion reactions or in decays of radioactive nuclei. As can be seen in Table II, solar neutrino fluxes are dominated by the pp neutrino and the ^{7}Be neutrino. Fluxes of ^{13}N neutrinos, ^{15}O neutrinos, and pep neutrinos are also not small. Solar neutrinos also have quite a wide spectrum. For $E_\nu \lesssim 0.4$ MeV, the solar neutrino spectrum is dominated by the pp neutrinos. For $E_\nu \gtrsim 1.74$ MeV, it is dominated by ^{8}B neutrinos. In between 0.4 and 1.74 MeV, major contributions are from ^{7}Be neutrinos, ^{13}N neutrinos, and ^{15}O neutrinos [36].

Solar electron neutrinos oscillate into muon neutrinos and tau neutrinos in propagation from the Sun to the Earth [37,38]. The probability of electron neutrinos surviving as electron neutrinos after propagation to the Earth depends on the energy of the neutrinos and on the matter density profile in the Sun. In [39], it was shown that the survival probability of solar electron neutrinos can be well described using a formula with an average density associated with the neutrino production in the Sun. Since eight types of solar neutrinos, as shown in Table II, have different production distribution in the Sun, the average survival probabilities are different for different types of solar neutrinos. For a solar neutrino of type k, we label P_k as the survival probability of the electron neutrinos after propagation to the Earth. P_k can be found in [39]. The survival probability also depends on the mass squared difference, Δm^2_{21}, and the vacuum mixing angle θ_{12}. When computing P_k, we use

$$\Delta m^2_{21} = 7.62 \times 10^{-5}\ \text{eV}^2, \qquad \sin^2\theta_{12} = 0.32. \tag{30}$$

In the previous section we find that in the scattering with bound electrons, solar neutrinos in a very wide energy range can contribute to the events with a final electron with a kinetic energy $E_k \approx 42$ keV. In particular, this means that neutrinos with energy less than $\frac{1}{2}(E_k + \sqrt{E_k^2 + 2E_k m_e})$, that is $\lesssim$126 keV for $E_k \approx 42$ keV, can contribute to the events with $E_k \approx 42$ keV.

Using the calculated neutrino fluxes and the energy spectrum for all eight types of neutrinos given in [36], we can compute the rate of events in the interested energy range, i.e., in the range $E_k \approx 42$ keV. The differential event rate of contributions of neutrinos with energy E_ν is computed as follows:

$$\frac{dR}{dE_\nu} = \frac{d\sigma_{\nu_e}(E_\nu)}{dE_k} N_e \sum_k F^k_\nu(E_\nu) P_k + \frac{d\sigma_{\nu_\mu}(E_\nu)}{dE_k} N_e \sum_k F^k_\nu(E_\nu)(1 - P_k), \tag{31}$$

where k runs over eight types of solar neutrinos, F^k_ν is the flux distribution of type k solar neutrinos, and N_e is the number of electrons in the Ru target. σ_{ν_e} and σ_{ν_μ} are the cross sections for the scattering of an electron neutrino and a muon neutrino, respectively. $P_k = P_k(E_\nu)$ is the survival probability of an electron neutrino as described above. $1 - P_k$ is the probability of solar electron neutrinos oscillating into muon neutrinos and tau neutrinos. Since the scattering of ν_μ and ν_τ with electrons is universal, we use σ_μ in Eq. (31). For simplicity, we neglect the Earth matter effect in our calculation, since it would lead to at most about 4% corrections for large energy solar neutrinos [39]. For solar neutrinos with energy less than about 1 MeV, the Earth matter effect would be smaller than 1% and can be safely neglected.

The differential cross section used in (31) is an average for the scattering with all electrons in the neutral Ru atom. It is written as

$$\frac{d\sigma_{\nu_e}}{dE_k} = \frac{1}{Z} \sum_l n_l \frac{d\sigma_l}{dE_k}, \tag{32}$$

where l runs over all states in Table I, n_l is the number of electrons in state l, and $Z = 44$ for a Ru atom. For electrons

TABLE II. Calculated solar neutrino flux [36]. Uncertainties of solar neutrino fluxes are shown in brackets.

Sources	Fluxes (10^{10} cm^{-2} s^{-1})	Energy (MeV)
pp	6.0 (±2%)	[0, 0.423]
pep	0.014(±5%)	1.44
hep	$8. \times 10^{-7}$	[0, 18.78]
^{7}Be	0.47(±15%)	0.861
^{8}B	5.8×10^{-4} (±37%)	[0, 16.40]
^{13}N	0.06 (±50%)	[0, 1.199]
^{15}O	0.05 (±58%)	[0, 1.732]
^{17}F	5.2×10^{-4}(±46%)	[0, 1.74]

in the M, N, and O shells, we approximate $d\sigma_l/dE_k$ to be the same as that of the scattering with a free electron at rest, as discussed in the last section. Similarly we have an expression for $d\sigma_{\nu_\mu}$.

The total rate is obtained after integrating Eq. (31) over E_ν. For 10 tons of ^{106}Ru, we obtain

$$R = 0.21 \times \frac{\Delta E_k}{10\ \text{eV}}\,\text{year}^{-1}. \tag{33}$$

We can see in Eq. (33) that if the energy of a final electron can be measured to a resolution of 10 eV, solar neutrinos would produce about 0.2 electron events in the scattering with electrons in 10 tons of ^{106}Ru target. In [3], it was shown that for θ, the mixing of the sterile neutrino DM to an electron neutrino, of order $\theta^2 = 10^{-6}$, the ν_s capture by ^{106}Ru can produce tens of events per year. Equation (33) says that background from the scattering with solar neutrinos allows us to measure θ^2 to a precision of 10^{-7} if the energy of the final electron can be measured to a precision of 10 eV. If the energy of the final electron can only be measured to a resolution of 100 eV, this background allows us to measure θ^2 to a precision of 10^{-6}.

In calculating the event rate, we find that the scattering with solar neutrinos of energy $\lesssim$126 keV gives a small contribution to the result given in Eq. (33). This is because (1) the cross section in this energy range is suppressed compared to that in the energy range $E_\nu \gtrsim 126$ keV, as can be seen in Figs. 4 and 5; and (2) the solar neutrinos in this energy range only account for about 7% of the total solar neutrino flux. We note that an electron, after passing out of the target, can lose energy and create a broadening of the spectrum. But this does not change our result in Eq. (33), because the event rate R varies very slowly with E_k. A spectrum broadening of a 10–100 eV level just gives rise to a mild redistribution of events in the original spectrum, and it would not change the estimate of a continuous spectrum in a range as wide as a few to around ten keV.

VI. CONCLUSION

In summary, we have studied in detail the scattering of solar neutrinos with bound electrons in Ru atoms. This study is helpful to clarify the background events caused by solar neutrinos in the search of keV scale sterile neutrino DM using a ^{106}Ru target.

We concentrate on the scattering of solar neutrinos with electrons in the $1s$, $2s$, and $2p$ states in a Ru atom. We find that for small E_ν, the scattering of neutrinos with a free electron at rest and the scattering with a bound electron can be quite different. For large E_ν, the difference tends to be small. For $E_\nu > m_e$, the difference tends to be negligible. For events of final electrons with a fixed kinetic energy, say $E_k \approx 42$ keV, we find that the scattering of a neutrino with a free electron at rest starts to contribute when $E_\nu \gtrsim 126$ keV. On the other hand, the scattering of a neutrino with a bound electron starts to contribute from values of E_ν much smaller than 126 keV. This means that the low energy part of the solar neutrino spectrum can contribute to the scattering. This part of the solar neutrino spectrum would be neglected when using the cross section of the scattering of neutrinos with free electrons at rest. Fortunately, solar neutrinos with energy $E_\nu \lesssim 126$ keV only account for about 7% of the total neutrino flux, and the scattering with bound electrons does not give a large difference compared to that computed using the scattering with free electrons at rest.

We estimate the event rate of electrons produced by the scattering of solar neutrinos with electrons in Ru atoms. We find that events of final electrons having $E_k \approx 42$ keV are 0.2 per year if the energy of the final electron can be measured to a precision of 10 eV. This allows us to search for the ν_s DM with a mixing of ν_s and ν_e at order $\theta^2 = 10^{-7}$. If the energy of the final electron can be measured to a precision of 100 eV, it allows us to search for the ν_s DM with a mixing of ν_s and ν_e at order $\theta^2 = 10^{-6}$. For 10 kg ^{3}T as used in [3] for the search of ν_s DM, the rate of this type of background event is about a thousand times smaller. It does not create a problem for the search of ν_s DM using a ^{3}T target. We find that for a larger energy resolution, the event rate of the background is larger. To avoid the pollution of this type of electron event in the search of sterile neutrino DM, we should have good energy resolution to suppress this type of background event.

ACKNOWLEDGMENTS

This work is supported by National Science Foundation of China (NSFC), Grants No. 11135009 and No. 11375065, and the Shanghai Key Laboratory of Particle Physics and Cosmology, Grant No. 11DZ2230700.

Note added.—Recently we received articles [40] which claim that the mixing angle $\boldsymbol{\theta}$ is strongly constrained by x-ray observation data to be $\boldsymbol{\theta^2} <$ a few $\times 10^{-8}$ for $\boldsymbol{m_s \approx 1-2\ \text{keV}}$. If it is a correct bound to apply to the result in [3] and the discussion in this article, the signal rate of capturing the keV scale sterile neutrino DM in the Universe would be much smaller and detecting this DM in the Universe using a target of radioactive nuclei would be much more difficult. However, the constraint in [40] makes a particular assumption on the thermal history of the early Universe, and it cannot be applied to models which have a dilution of the density of sterile neutrino DM after the sterile neutrino DM has been produced in the early Universe [3,12,19]. In this article, we discuss the topic of the detection of sterile neutrino DM, and it is not the purpose of the present article to discuss situations in different models of this DM candidate. So we work with a much more model-independent bound from the analysis of x-ray observation data [13,31] which does not assume a thermal history of the early Universe and is orders of magnitude weaker than the bound in [40].

[1] J. Sommer-Larsen and A. Dolgov, Astrophys. J. **551**, 608 (2001); P. Colin, V. Avila-Reese, and O. Valenzuela, Astrophys. J. **542**, 622 (2000).

[2] C. Destri, H. J. de Vega, and N. G. Sanchez, New Astron. **22**, 39 (2013); Astropart. Phys. **46**, 14 (2013).

[3] W. Liao, Phys. Rev. D **82**, 073001 (2010).

[4] P. L. Biermann, H. J. de Vega, and N. G. Sanchez, arXiv: 1305.7452.

[5] T. Asaka, S. Blanchet, and M. Shaposhnikov, Phys. Lett. B **631**, 151 (2005).

[6] For recent reviews, see A. Merle, Int. J. Mod. Phys. D **22**, 1330020 (2013); M. Drewes, Int. J. Mod. Phys. E **22**, 1330019 (2013).

[7] S. Dodelson and L. W. Windrow, Phys. Rev. Lett. **72**, 17 (1994).

[8] A. D. Dolgov and S. H. Hansen, Astropart. Phys. **16**, 339 (2002); K. Abazajian, G. M. Fuller, and M. Patel, Phys. Rev. D **64**, 023501 (2001); K. Abazajian, G. M. Fuller, and W. H. Tucker, Astrophys. J. **562**, 593 (2001).

[9] A. Boyarsky, J. Lesgourgues, O. Ruchayskiy, and M. Viel, Phys. Rev. Lett. **102**, 201304 (2009).

[10] M. Shaposhnikov and I. Tkachev, Phys. Lett. B **639**, 414 (2006).

[11] K. Petraki and A. Kusenko, Phys. Rev. D **77**, 065014 (2008).

[12] F. Bezrukov, H. Hettmansperger, and M. Lindner, Phys. Rev. D **81**, 085032 (2010).

[13] A. Boyarsky, A. Neronov, O. Ruchayskiy, M. Shaposhnikov, and I. Tkachev, Phys. Rev. Lett. **97**, 261302 (2006); A. Boyarsky, J.-W. den Herder, A. Neronov, and O. Ruchayskiy, Astropart. Phys. **28**, 303 (2007).

[14] A. Boyarsky, J. Nevalainen, and O. Ruchayskiy, Astron. Astrophys. **471**, 51 (2007).

[15] A. Boyarsky, D. Iakubovskyi, O. Ruchayskiy, and V. Savchenko, Mon. Not. R. Astron. Soc. **387**, 1361 (2008).

[16] A. Boyarsky, J. Lesgourgues, O. Ruchayskiy, and M. Viel, J. Cosmol. Astropart. Phys. 05 (2009) 012.

[17] A. Boyarsky, O. Ruchayskiy, and D. Iakubovskyi, J. Cosmol. Astropart. Phys. 03 (2009) 005.

[18] M. Shaposhnikov, Nucl. Phys. **B763**, 49 (2007).

[19] T. Asaka, M. Shaposhnikov, and A. Kusenko, Phys. Lett. B **638**, 401 (2006).

[20] M. Lindner, A. Merle, and V. Niro, J. Cosmol. Astropart. Phys. 01 (2011) 034.

[21] C.-Q. Geng and R. Takahashi, Phys. Lett. B **710**, 324 (2012).

[22] L. Canetti, M. Drewes, and M. Shaposhnikov, Phys. Rev. Lett. **110**, 061801 (2013).

[23] D. J. Robinson and Y. Tsai, J. High Energy Phys. 08 (2012) 161.

[24] D. Boyanovsky, Phys. Rev. D **78**, 103505 (2008).

[25] A. Boyarsky, D. Iakubovskyi, and O. Ruchayskiy, Phys. Dark Univ. **1**, 136 (2012).

[26] Y. F. Li and Z. Z. Xing, J. Cosmol. Astropart. Phys. 08 (2011) 006.

[27] Y. F. Li and Z. Z. Xing, Phys. Lett. B **695**, 205 (2011).

[28] H. de Vega, O. Moreno, E. Moya de Guerra, M. R. Medrano, and N. G. Sánchez, Nucl. Phys. **B866**, 177 (2013).

[29] F. Bezrukov and M. Shaposhnikov, Phys. Rev. D **75**, 053005 (2007).

[30] S. Ando and A. Kusenko, Phys. Rev. D **81**, 113006 (2010).

[31] A. Boyarsky, O. Ruchayskiy, and M. Shaposhnikov, Annu. Rev. Nucl. Part. Sci. **59**, 191 (2009).

[32] *CRC Handbook of Chemistry and Physics*, edited by David R. Lide (CRC Press, Boca Raton, FL, 2005).

[33] J. A. Bearden and A. F. Burr, Rev. Mod. Phys. **39**, 125 (1967).

[34] J. Beringer *et al.* (Particle Data Group), Phys. Rev. D **86**, 010001 (2012).

[35] M. A. Coplan, J. Moore, and J. Doering, Rev. Mod. Phys. **66**, 985 (1994).

[36] J. N. Bahcall, *Neutrino Astrophysics* (Cambridge University Press, Cambridge, England, 1989); see also online data at http://www.sns.ias.edu/~jnb/SNdata/sndata.html.

[37] L. Wolfenstein, Phys. Rev. D **17**, 2369 (1978); L. Wolfenstein, in *Neutrino-78* (Purdue University, West Lafayette, Indiana, 1978), Chap. 3–6.

[38] S. P. Mikheyev and A. Yu. Smirnov, Yad. Fiz. **42**, 1441 (1985) [Sov. J. Nucl. Phys. **42**, 913 (1985)]; Nuovo Cimento Soc. Ital. Fisc. C **9**, 17 (1986); S. P. Mikheyev and A. Yu. Smirnov, Zh. Eksp. Teor. Fiz. **91** (1986) [Sov. Phys. JETP, **64**, 4 (1986)] (reprinted in *Solar Neutrinos: The First Thirty Years*, edited by J. N. Bahcall *et al.*).

[39] P. C. de Holanda, W. Liao, and A. Yu. Smirnov, Nucl. Phys. **B702**, 307 (2004).

[40] M. Loewenstein, A. Kusenko, and P. L. Biermann, Astrophys. J. **700**, 426 (2009); M. Loewenstein and A. Kusenko, Astrophys. J. **751**, 82 (2012).